CONFOCAL MICROWAVE IMAGING FOR BREAST TUMOR DETECTION: A STUDY OF RESOLUTION AND DETECTION ABILITY

E.C. Fear and M.A. Stuchly
Department of Electrical and Computer Engineering, University of Victoria, Victoria, BC, Canada

Abstract-**Confocal microwave imaging (CMI) is a recently introduced method of breast tumor detection that utilizes techniques adapted from ground penetrating radar for mine detection. Initial feasibility studies performed with simulated data indicate that CMI is a promising method for tumor detection and localization. In this paper, we explore the detection ability and resolution of the system. The detection ability is examined by imaging tumors of small diameter, while resolution is investigated by imaging 2 tumors located in close proximity. Results indicate that tumors located 3 cm deep and of 3-mm diameter and greater are detected. Resolution is estimated to be 1 cm for two 6-mm diameter tumors.**
Keywords - **Microwave imaging, breast cancer, resolution**

I. INTRODUCTION

Breast cancer is a health concern for many women, and early detection of this disease is important for comfortable and effective treatment. The gold standard method of early detection, mammography, involves x-ray imaging a compressed breast. A recent study of breast screening programs in Canada indicated a positive predictive value of less than 10% for mammography [1]. That is, less than 10% of abnormalities on mammograms corresponded to malignancies. The need for additional information to aid in diagnosis has generated interest in applying alternative methods of imaging to breast tumor detection.

Recently proposed confocal microwave imaging (CMI) has shown promising results for breast tumor detection [2,3]. The physical basis of tumor detection with CMI is the contrast in electrical properties of normal breast tissue and malignant breast tumors. CMI involves illuminating the breast with an ultra-wideband pulse of microwaves, and recording reflections at the illuminating antenna. The antenna is physically scanned to a number of different locations, and the data acquisition process is repeated at each position. Thus, the breast is illuminated by and reflections are recorded at each member of an array of antennas. To form images, the synthetic focus of the array is scanned systematically through the breast. Due to the use of ultra-wideband signals, synthetic focussing is accomplished by computing the time delay from each antenna to the focal point. The corresponding time-delayed data are summed, forming the contribution to the image at the focal point location. Returns from strongly scattering objects add coherently when the focal point corresponds to their location; at other points in the image, clutter adds incoherently and is reduced. As normal breast tissue is relatively translucent and tumors are strongly scattering at the frequencies of interest, tumor detection results from the contrast in electrical properties of normal and malignant breast tissues.

We are investigating a cylindrical CMI system, in which the woman to be scanned lies on her stomach with the breast extending through a hole in the examination table [4,5]. Antennas encircle the breast, and are located at a distance from the skin. Preliminary computational results indicate successful detection and localization of small tumors. In this paper, we explore the detection ability and resolution of the simulated system.

II. METHODOLOGY

A. Models and simulations

A simple cylindrical breast model is used to investigate resolution and detection ability. Fig. 1 shows a cross-section of the 6.8-cm diameter model, which consists of breast tissue surrounded by a 2-mm thick layer of skin. The breast tissue has random variations in electrical properties of up to ±10% over 4 mm cubes. One or more spherical tumors of diameters ranging from 2 to 6 mm are embedded in the breast tissue. The breast is illuminated with a resistively loaded dipole antenna [5] located 1 cm from the breast skin. Both breast model and antenna are immersed in a lossless immersion medium with properties similar to those of breast tissue. The electrical properties of the materials in the model are shown in Table 1.

The finite difference time domain method simulates the illumination of the breast model with an ultra-wideband pulse [6]. The time signature of the pulse is a differentiated Gaussian, and frequency content (greater than 10% of the maximum amplitude) ranges from 0.2 to 10 GHz. Only one antenna is present in any simulation. To form the array, the antenna is moved to a set of physical locations, and a simulation is performed at each of these locations. In most cases reported in this paper, the antenna is scanned to 10 positions, equally spaced on a circular path located 1 cm from the breast.

To evaluate detection ability, tumors of diameters 2, 3, 4 and 6-mm and located approximately 3 cm deep in the breast are investigated. First, reflections at 10 antenna locations are recorded from a model with a 6-mm diameter tumor and a model without a tumor. These returns are subtracted to isolate the tumor response recorded at each antenna. The 6-mm diameter tumor is replaced with 2, 3, and 4-mm diameter tumors, and reflections at the antennas located closest to and furthest from the tumor are recorded. The reflections are similar in shape, but different in amplitude. Therefore, the tumor response at the 10 antennas is approximated for the 2, 3

Report Documentation Page

Report Date	Report Type	Dates Covered (from... to)
25OCT2001	N/A	-

Title and Subtitle Confocal Microwave Imaging for Breast Tumor Detection: A Study of Resolution and Detection Ability	**Contract Number**
	Grant Number
	Program Element Number
Author(s)	**Project Number**
	Task Number
	Work Unit Number
Performing Organization Name(s) and Address(es) Department of Electrical and Computer Engineering, University of Victoria, Victoria, BC, Canada	**Performing Organization Report Number**
Sponsoring/Monitoring Agency Name(s) and Address(es) US Army Research Development & Standardization Group (UK) PSC 803 Box 15 FPO AE 09499-1500	**Sponsor/Monitor's Acronym(s)**
	Sponsor/Monitor's Report Number(s)

Distribution/Availability Statement
Approved for public release, distribution unlimited

Supplementary Notes
Papers from the 23rd Annual International conference of the IEEE Engineering in Medicine and Biology Society, October 25-28, 2001, held in Istanbul, Turkey. See also ADM001351 for entire conference on cd-rom., The original document contains color images.

Abstract

Subject Terms

Report Classification unclassified	**Classification of this page** unclassified
Classification of Abstract unclassified	**Limitation of Abstract** UU

Number of Pages
4

and 4-mm diameter tumors by scaling the 6-mm diameter tumor response. The scaled responses are added to the tumor-free reflections to simulate the total reflection from the tumor-bearing breast models. This allows for rapid insight into detection ability without excessive computational cost, as each simulation requires 6.7 hours on the Minerva High Performance Computing Facility at the University of Victoria (1 processor of an 8 node IBM RS/6000 SP running at 375 MHz). After estimating the smallest tumor detected, full simulations are performed to verify the approximated results.

To test resolution, two tumors are embedded in the breast model. The scenarios investigated are two 4-mm diameter tumors with centers separated by 8 mm and located equal distances from the breast model center. Two 6-mm diameter tumors with center separations of 7.2 mm and 10 mm are also examined. The 4-mm diameter tumors separated by 8 mm are illuminated at 10 and 20 antenna locations; the 6-mm diameter tumors are illuminated at 10 antenna locations.

B. Image reconstruction

The first step in image reconstruction is calibration, which involves subtracting the response recorded without a breast model present. Next, the dominant reflections from the skin are reduced by aligning the skin reflections, then subtracting the average of the aligned data set from each reflection. The skin-subtracted data set is integrated to transform the mid-point of the excitation signal from a zero to a maximum. Radial spreading compensation accounts for the 1/r decay of a spherical wave as it propagates from the source. In this case, multiplication by r^2 is used to compensate for the outgoing and return paths. Computing the time delay from each antenna location to the focal point of interest, and summing the corresponding portions of each signal synthetically focuses the resulting data set. The focal point is scanned to a new location, and this procedure is repeated for all points inside of the antenna array. Images are displayed by taking the energy of the resulting matrix.

C. Measures of detection ability and resolution

Detection ability is evaluated with the signal-to-clutter ratio. This compares the maximum tumor response to the maximum response in the image outside of the tumor. With a signal-to-clutter ratio of 1.5 dB, the tumor is easily detected with visual inspection. Resolution is evaluated by visual inspection.

III. Results

A. *Detection ability*

Initially, scaled reflections from a 6-mm diameter tumor approximate reflections from smaller tumors. Fig. 2 compares the normalized reflections from tumors of diameters 2 to 6 mm. Similarities in the initial tumor responses indicate that the approximation is reasonable, however larger responses are introduced in later time, increasing clutter. The 6-mm diameter tumor responses are scaled by the following factors to represent smaller tumors: 0.47 (4 mm), 0.23 (3 mm), and 0.08 (2 mm).

Images are reconstructed with computed data for the 6-mm diameter tumor (Fig. 3), and approximated data for 2, 3 and 4 mm diameter tumors. The signal-to-clutter ratios are 4.0 dB (6 mm), 1.5 dB (4 mm) and -1.8 dB (3 mm). The 2-mm diameter tumor is not visually detected. As the 3-mm diameter tumor is evident in the image reconstructed with approximate data, results are computed for this case. The image reconstructed with the computed data is shown in Fig. 4, and has signal-to-clutter ratio of –2.2 dB.

B. Resolution

Resolution is first investigated by imaging two 4-mm diameter tumors separated by 8 mm. Images reconstructed with 10 and 20 antennas are shown in Fig. 5 and 6. One tumor is located at the red response near the center of the breast, while the white circle shows the location of the second tumor. Next, 6-mm diameter tumors are investigated. With a tumor separation of 7.2 mm, only 1 tumor response is evident on the image. Images of two tumors separated by 1 cm are shown in Fig. 7, and a second tumor response is evident.

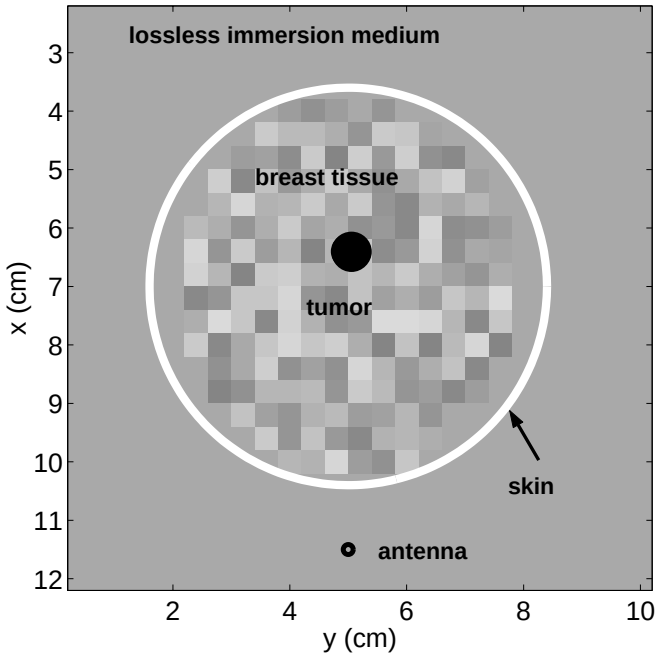

Fig. 1. Cross-section through cylindrical breast model, indicating materials and location of antenna relative to model.

TABLE I
ELECTRICAL PROPERTIES OF MATERIALS IN BREAST MODEL

Material	Relative Permittivity	Conductivity (S/m)
Breast tissue	9	0.4
Skin	36	4
Tumor	50	4
Immersion liquid	9	0

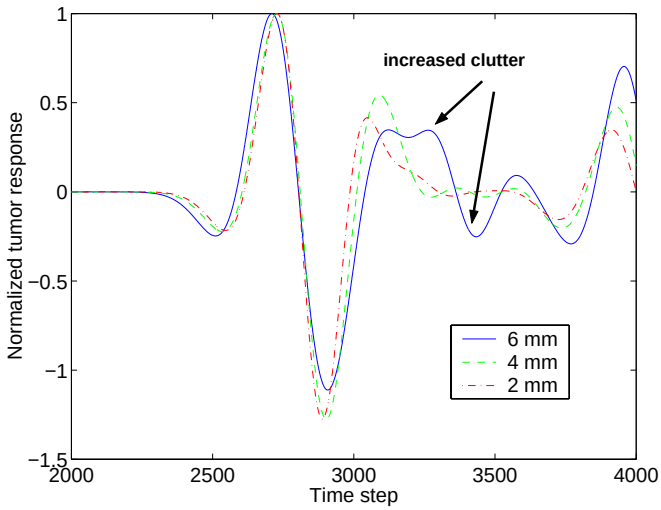

Fig. 2. Normalized tumor response for 2 to 6 mm diameter tumors.

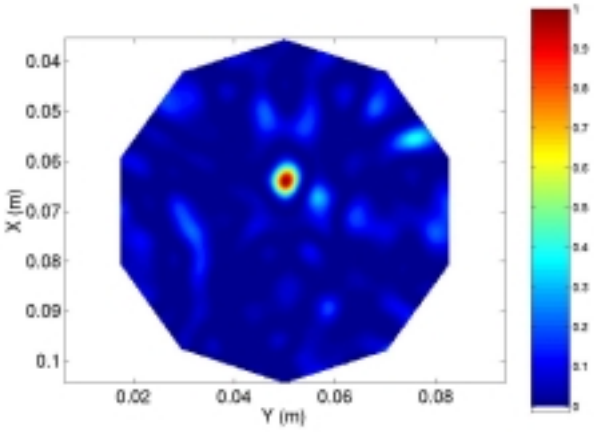

Fig. 3. Image of breast model with 6-mm diameter tumor at x=0.064, y=0.05.

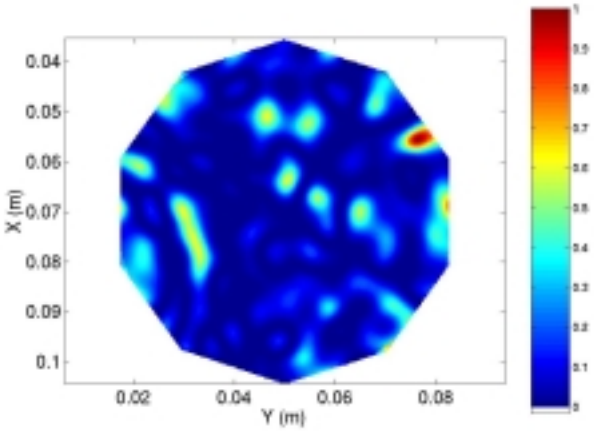

Fig. 4. Image of breast model with 3-mm diameter tumor at x=0.064, y=0.05.

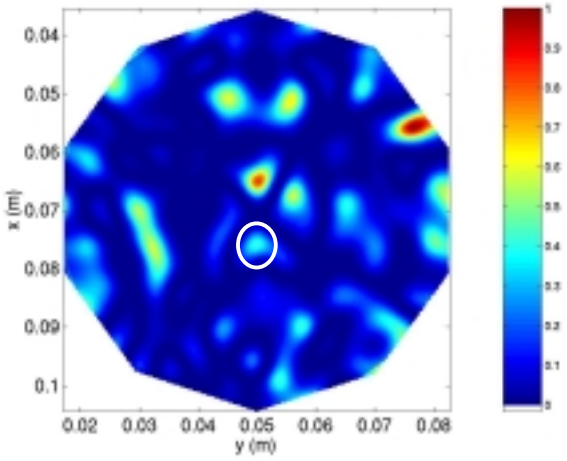

Fig. 5. Image of breast model containing two 4-mm diameter tumors. Data recorded at 10 antennas are used to form the image. The white circle indicates the physical location of the second tumor.

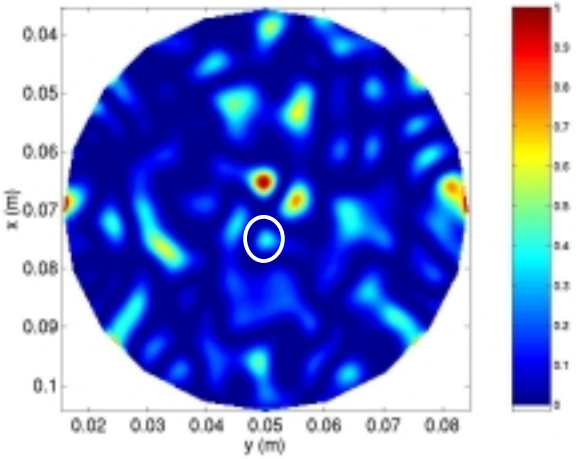

Fig. 6. Image of breast model containing two 4-mm diameter tumors. Data recorded at 20 antennas are used to form the image. The white circle indicates the physical location of the second tumor.

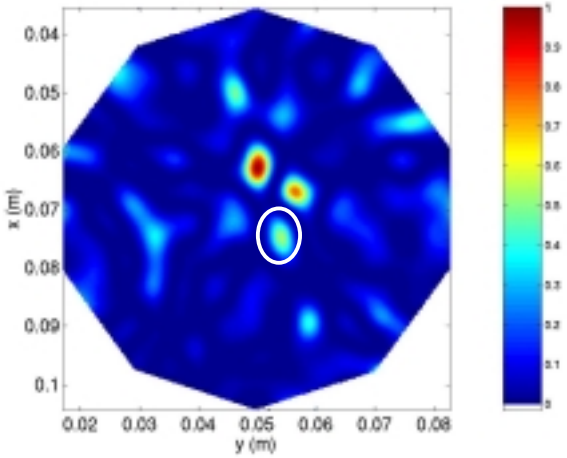

Fig. 7. Image of breast model containing two 6-mm diameter tumors. Data recorded at 10 antennas are used to form the image. The white circle indicates the physical location of the second tumor.

IV. Discussion

A. Detection ability

Insight into detection ability may be obtained by approximating the tumor response. This is indicated by comparison of computed and approximated data for the 3-mm diameter tumor. The images formed with computed and approximated data are similar, however the signal-to-clutter ratio is smaller with the computed data. The 3-mm diameter tumor is visually apparent in the computed image, although clutter dominates this image. Tumors of 3-mm diameter and greater are detected with mammography [7], so CMI has the potential to provide complementary information for lesions of interest in mammography. The smaller tumors examined here are at depths of 3 cm in the breast. With increased depth, it is likely more challenging to detect such small tumors.

B. Resolution

The initial resolution study (Fig. 5) shows one tumor response, while two 4-mm diameter tumors are present in the model. With more antennas, the signal-to-clutter ratio appears to improve and a second tumor response is evident. The location of the second tumor response does not, however, correspond to the physical tumor location. Inspection of Figs. 3 and 4 demonstrates the presence of clutter at the location of the second tumor response in Fig. 6. Clutter is not present at the physical location of the second tumor. In Fig. 6, a response is evident at the physical location of the second tumor. However, this is smaller than the response resulting from the addition of the tumor response and clutter. As shown in the study of detection ability, detecting small tumors is challenging. With multiple tumors present, reduced responses are received from the tumor furthest from a given antenna (i.e. reflections are predominantly received from the tumor closest to the antenna). Fig. 7 demonstrates that improved results are obtained with larger tumors due to their more significant reflections. The response due to addition of the clutter and tumor reflections persists, however the response at the physical location of the second tumor is larger. For this CMI system with tumors of 6 mm diameter located approximately 3 cm below the skin, resolution is estimated as 1 cm. Although the two tumors are not clearly localized in Figs. 6 and 7, responses in the images indicate the presence of at least one strongly scattering object.

C. Resolution and detection

Although this CMI system is estimated to have resolution of 1 cm, detection of tumors smaller than 1 cm is achieved. This suggests that fine resolution may not be required to detect small tumors with CMI. The resolution study suggests that a sufficient number of spatial samples (antenna locations) is required to image more complex objects correctly, especially as the targets of interest decrease in size. In addition to the images in Figs. 3 to 7, difference images are examined for both resolution and detection capability studies. These images are obtained by subtracting images of tumor-free and tumor-bearing models. In all cases, small tumors are detected and multiple tumors are clearly evident at their physical locations. This suggests that subtraction of right and left breast images may be useful, however further investigation with more realistic breast models is required to evaluate the clinical feasibility of this approach. The results in both studies also demonstrate the need for effective clutter reduction algorithms to improve detection and reduce false alarms. Finally, the resolution and detection capability estimated here must be evaluated with more realistic breast models and experiments.

V. Conclusion

This study indicates that CMI appears capable of detecting tumors of 3-mm diameter and greater at depths in the breast tissue of less than 3 cm. Resolution is estimated at 1 cm, and appears to depend on the number of antennas used to form the image, as well as the size of target. Future investigations with more realistic models and development of effective clutter reduction algorithms are required to move CMI further towards clinical implementation.

References

[1] D. Paquette, J. Snider, F. Bouchard, I. Olivotto, H. Bryant, K. Decker, G. Doyle, "Performance of screening mammography in organized programs in Canada in 1996," *CMAJ*, vol. 163 (9), 2000, pp. 1133-8.

[2] S.C. Hagness, A. Taflove and J.E. Bridges, "Two-dimensional FDTD analysis of a pulsed microwave confocal system for breast cancer detection: fixed-focus and antenna-array sensors", *IEEE Transac. Biomed. Eng.*, vol. 45, Dec. 1998, pp. 1470-1479.

[3] S.C. Hagness, A. Taflove and J.E. Bridges, "Three-dimensional FDTD analysis of pulsed microwave confocal system for breast cancer detection: design of an antenna-array element", *Transac. Antennas Propag.*, vol. 47, May 1999, pp. 783-791.

[4] E.C. Fear and M.A. Stuchly, "Microwave detection of breast cancer," *IEEE Transactions on Microwave Theory and Techniques*, vol. 48, Nov. 2000, pp. 1854-1863.

[5] E.C. Fear and M.A. Stuchly, "Microwave system for breast tumor detection", *IEEE Microwave and Guided Wave Letters*, vol. 9, Nov. 1999, pp. 740-742.

[6] A. Taflove and S.C. Hagness, *Computational electrodynamics: the finite difference time domain method*, 2nd ed., Artech House, Norwood, MA, 2000.

[7] M. Sabel and H. Aidringer, "Recent developments in breast imaging", *Phys. Med. Biol.*, vol. 41, 1996, pp. 315-368.